



1           **Is Annual Recharge Coefficient a Valid Concept in Arid and Semi-Arid Region?**

2

3

4

5           Yiben Cheng<sup>a\*</sup>, Hongbin Zhan<sup>b\*</sup>, Wenbin Yang<sup>a\*</sup>, Hongzhong Dang<sup>a</sup>, Wei Li<sup>a</sup>

6

7

<sup>a</sup> Institute of Desertification Studies,

8

Chinese Academy of Forestry,

9

Haidian District, Beijing 100093, P. R. China ([chengyiben07@gmail.com](mailto:chengyiben07@gmail.com))

10

11

<sup>b</sup>Department of Geology & Geophysics,

12

Texas A&M University,

13

College Station, TX 77843-3115, USA. ([zhan@geos.tamu.edu](mailto:zhan@geos.tamu.edu))

14

15

\*Co-corresponding authors

16

17

18

19

20



21 **Abstract.** Deep soil recharge (DSR) (at depth more than 200 cm) is an important part of water  
22 circulation in arid and semi-arid regions. Quantitative monitoring of DSR is of great importance  
23 to assess water resources and to study water balance in arid and semi-arid regions. This study  
24 used a typical bare land on the Eastern margin of Mu Us Sandy Land in the Ordos basin of China  
25 as an example to illustrate a new lysimeter method of measuring DSR to examine if the annual  
26 recharge coefficient is valid or not in the study site, where the annual recharge efficient is the  
27 ratio of annual DSR over annual total precipitation. Positioning monitoring was done on  
28 precipitation and DSR measurements underneath mobile sand dunes from 2013 to 2015 in the  
29 study area. Results showed that use of an annual recharge coefficient for estimating DSR in bare  
30 sand land in arid and semi-arid regions is questionable and could lead to considerable errors. It  
31 appeared that DSR in those regions was influenced by precipitation pattern, and was closely  
32 correlated with spontaneous strong precipitation events (with precipitation greater than 10 mm)  
33 other than the total precipitation. This study showed that as much as 42% of precipitation in a  
34 single strong precipitation event can be transformed into DSR. During the observation period,  
35 the maximum annual DSR could make up to 24.33% of the annual precipitation. This study  
36 provided a reliable method of estimating DSR in sandy area of arid and semi-arid regions, which  
37 is valuable for managing groundwater resources and ecological restoration in those regions. It  
38 also provided strong evidence that the annual recharge coefficient was invalid for calculating  
39 DSR in arid and semi-arid regions. This study shows that DSR is closely related to the strong  
40 precipitation events, rather than to the average annual precipitation.

41 **Key words:** Deep soil recharge, deep soil infiltrometer, sandy land, new apparatus, rainfall,  
42 lysimeter

43



#### 44 **Introduction**

45 Recharge is an important source of groundwater budget and it is also a fundamental process  
46 that links the surface hydrological processes (e.g. precipitation), vadose zone process (e.g.  
47 infiltration and soil moisture dynamics), and the saturated zone process (e.g. groundwater flow)  
48 (Sanford, 2002;McWhorter and Sunada, 1977). How to accurately estimate recharge remains a  
49 persistent challenge and an active research topic in the hydrological science community over  
50 many decades (Gee and Hillel, 1988;Scanlon, 2013;Sanford, 2002). It is generally accepted that  
51 recharge is correlated to the precipitation in some fashions, and many studies adopt the concept  
52 of a recharge coefficient (Turkeltaub et al., 2015;Kalbus et al., 2006;Allocca et al., 2014), which  
53 is the ratio of the actual recharge to the precipitation, to estimate the recharge (Fiorillo et al.,  
54 2015;Allocca et al., 2014). The magnitude of such a recharge coefficient is controlled by a  
55 complex interplay of multiple factors such as moisture dynamics in the vadose zone  
56 (Schymanski et al., 2008), depth to the water table, vegetation, etc., and the recharge coefficient  
57 is often regarded as a temporally invariant value at a given location (Fiorillo et al., 2015;Min et  
58 al., 2017;Vauclin et al., 1979). Specifically, it is assumed to be primarily controlled by the total  
59 precipitation, not too much by the temporal fluctuation of precipitation events (Hickel and Zhang,  
60 2006;Acworth et al., 2016). In this study, we will challenge the concept of using a constant  
61 recharge coefficient to estimate the recharge in arid and semi-arid regions based on a multi-year  
62 field investigation.

63 As water tables in many arid and semi-arid regions are relatively deep (greater than 2  
64 meters below ground surface) (Williams, 1999;Soylu et al., 2011), recharge in those regions is  
65 named Deep Soil Recharge (DSR), which will be the concern of this study. DSR could ease the  
66 demand of sand-fixing vegetation on moisture during extremely dry seasons (Zhang et al.,



67 2001;Shou et al., 2016) , and it reduces water deficit, sustains life activities, and helps the  
68 vegetation to live through extreme droughts (Zhang et al., 2004). In this sense, DSR is an  
69 important factor of water cycle in arid and semi-arid regions (Adolph, 1947), and it could also  
70 provide much needed references for the stability analysis of sand-fixing vegetation (Li et al.,  
71 2004;Li et al., 2014). In the following, we will briefly review the existing methods of estimating  
72 DSR.

73 In general, there are three methods of measuring DSR in arid and semi-arid regions. The  
74 first is an empirical approach which assigns a constant recharge coefficient associated with a  
75 certain precipitation event (Allison et al., 1994;Jiménez-Martínez et al., 2010). The empirical  
76 approach is simple to use but it lacks a rigorous theoretical base, and the recharge coefficient has  
77 to be calibrated through a groundwater flow model in the region, which is often not available.

78 The second is a modeling approach involving numerical models such as HYDRUS  
79 (Šimůnek et al., 2012), SWAT (Arnold et al., 2012), UNSATH (Fayer, 2000), SWIM  
80 (Krysanova et al., 2005), SWAP (van Dam, 2000) to calculate DSR. Detailed water balance  
81 models can be used for irrigated agriculture, but they usually cannot predict evapotranspiration  
82 accurately, especially when plants suffer seasonal water stress and plants cover is sparse (Gee  
83 and Hillel, 1988). When recharge is estimated as residual in water balance models, it can cause  
84 miscalculation as much as an order of magnitude (Scanlon, 2013;Voeckler et al., 2014). When  
85 using soil water flow models with measured or estimated soil hydraulic conductivities and  
86 tension gradients, similar miscalculation can also occur (Nyman et al., 2014;Gee and Hillel,  
87 1988). In addition, the modeling usually involves upscaling of parameter values over a spatially  
88 and temporally discretized mesh from measurements which are made on specific moments and  
89 locations. Such an upscaling process is not always easy to execute and it could sometimes lead to



90 serious errors. This is particularly true for arid and semi-arid regions where most precipitation  
91 may be episodic (occurring in short and unpredictable events) (Modarres and da Silva,  
92 2007;Zhou et al., 2016), and may be confined to restricted portions of the area (Gee and Hillel,  
93 1988).

94 The third includes a cluster of experimental techniques such as isotopic tracer (Klaus and  
95 McDonnell, 2013), water flux (Katz et al., 2016), and lysimeter (Scanlon, 2013). Among them,  
96 lysimeters are instruments that directly measure the hydrological cycle in infiltration, runoff and  
97 evaporation. Generally, this equipment is located in an open observation field or as a controlled  
98 device, working either solely or in groups (Good et al., 2015). In a typical lysimeter, soil are  
99 filled into a column surrounded by impermeable lateral boundaries thus water can only enter or  
100 leave the column from upper or lower boundaries (Duncan et al., 2016;Fritzsche et al., 2016). A  
101 drainage system is usually placed at the bottom (Glenn et al., 2013). The depth of soil in the  
102 column depends on the experimental purpose. Experiments can be done with the same type of  
103 soil at different depths in a single column, or in different columns but at the same depth. The soil  
104 surface can be cultivated with different crops or left alone as bare land. Observation can be  
105 recorded with weight or volume of water.

106 Application of above-mentioned methods for assessing DSR in arid and semi-arid regions  
107 has met a variety of challenges, primarily due to the fact that precipitation events often happen in  
108 the form of short pulses with highly variable intensity (Collins et al., 2014). The intermittent and  
109 unpredictable characteristics of precipitation events lead to highly variable moisture and nutrient  
110 levels in the soils (Beatley, 1974;Huxman et al., 2004). It is unclear how the precipitation  
111 amount, time, and interval will affect the water moisture of arid and semi-arid regions, especially  
112 the change of deep soil water storage.



113 In this study, a new type of lysimeter is designed to accurately measure the amount of DSR  
114 in arid and semi-arid regions. With the help of a three-year (2013-2015) field investigation with  
115 this new lysimeter, one can answer the following question: Is the concept of an annual recharge  
116 coefficient valid or not for estimating DSR at a given location in an arid and semi-arid region?  
117 Before the introduction of this new type of lysimeter, it is necessary to briefly explain the  
118 challenges faced by the conventional lysimeter for studying DSR in arid and semi-arid regions.

## 119 **2. Design of the new lysimeter for DSR measurement**

### 120 **2.1. Problems with the conventional lysimeter methods in arid and semi-arid regions**

121 Lysimeters have been used to access the amount of water consumed by vegetation for more  
122 than three hundred years (Howell et al., 1991). The type of lysimeter that is specifically designed  
123 to measure evapotranspiration (ET), called precision weighing lysimeter, has been developed  
124 within the past six decades. In order to suit different requirements and needs, there are various  
125 designs of weighing lysimeters, with surface areas ranging from 1.0 m<sup>2</sup> to over 29 m<sup>2</sup> (Howell et  
126 al., 1991). The stored media mass and the type of scale such as diameter and height, are factors  
127 on which the accuracy of ET measurement depends, and many lysimeters have accuracies better  
128 than 0.05 mm (Howell et al., 1991). Figure 1A shows the schematic diagram of a conventional  
129 lysimeter installation in the field. It is basically a weight meter of soil with an open upper  
130 boundary at ground surface and a perforated bottom boundary and impermeable vertical side  
131 walls. The typical depth of lysimeters varies from 0.2 m to 2 m, but is rarely greater than 2.5 m  
132 (Howell et al., 1991). The horizontal cross-section area is usually in the range of 1 m<sup>2</sup> to 29 m<sup>2</sup>.  
133 Precipitated water can freely infiltrate into the soil from the top and downward flow of water at  
134 the bottom of the lysimeter is collected (through the perforation) as a function of time to  
135 calculate the recharge. Alternatively, the weight of combined water and soil inside the lysimeter



136 can be accurately measured using a weight gauge to reflect any soil moisture change. Such  
137 information, combined with infiltration or evaporation at the surface, can yield the information  
138 of downward water flux at the depth of lysimeter.

139 The following issues deserve special attention when applying the conventional lysimeter for  
140 measuring recharge. Firstly, soil layers are inevitably disturbed when installing the instrument,  
141 so the result may not reflect the actual recharge in native (undisturbed) soils (Weihermüller et al.,  
142 2007) . Secondly, the cost is too high to use multiple lysimeters to observe large-scale infiltration  
143 (Stessel and Murphy, 1992). Thirdly, when precipitation strength is relatively light and  
144 concentrated, a large lysimeter cannot sensitively and rapidly measure DSR (Goldhamer et al.,  
145 1999; Farahani et al., 2007). The conventional lysimeter often cannot answer the following  
146 questions: To what soil layer can different levels of precipitations infiltrate? How much is the  
147 infiltration amount under different levels of precipitation? (Gee and Hillel, 1988; Ogle and  
148 Reynolds, 2004).

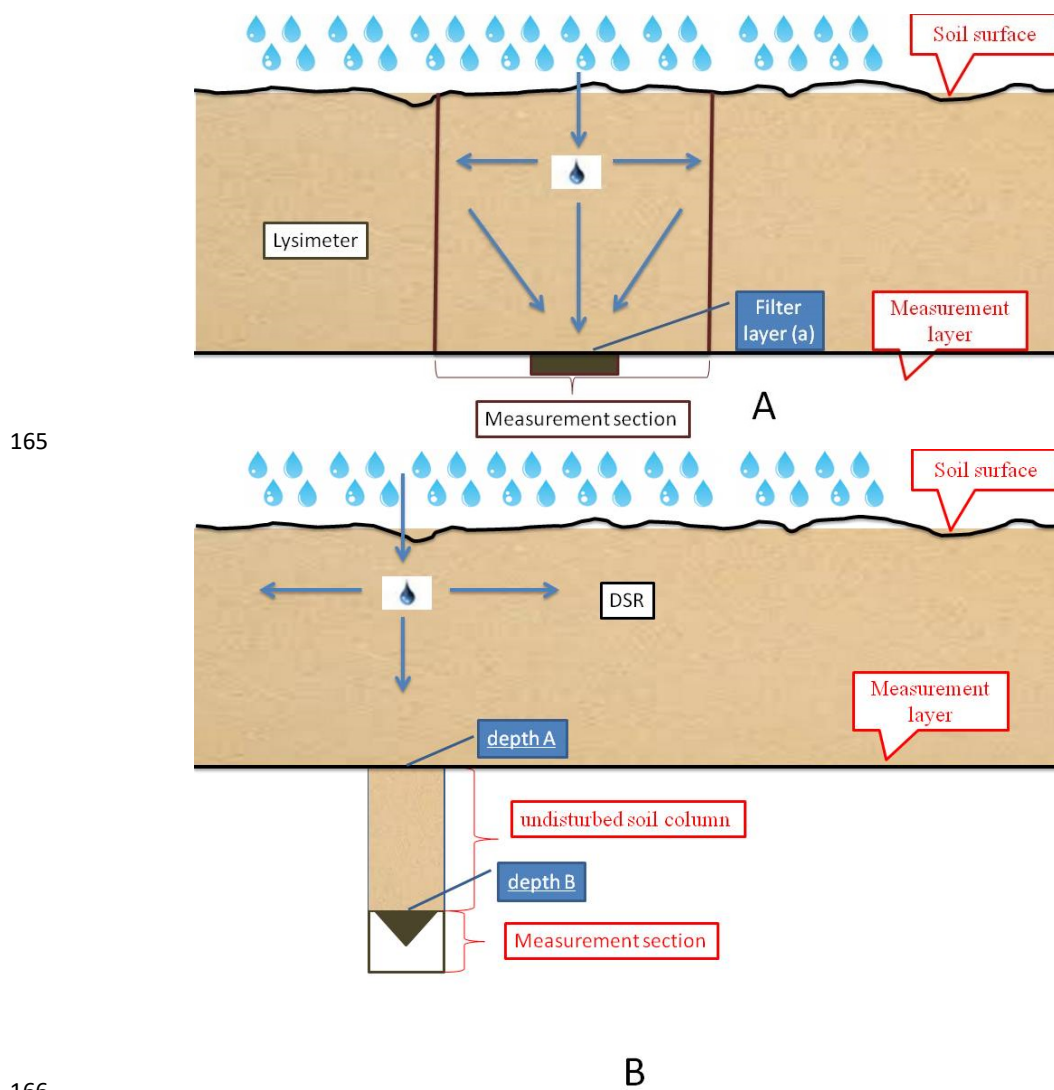
149 The conventional lysimeter as shown in Figure 1A may meet additional challenges when  
150 applied to arid and semi-arid regions. Firstly, the water table depths in arid and semi-arid regions  
151 may be much greater than the maximal depth of a conventional lysimeter (2.5 m). For instance,  
152 in Chagan Nur, southeast of Mu Us sandy land in the Ordos basin of China, the water table depth  
153 was found to be greater than 4 m. In the Gobi desert, the water table was reported to be at least  
154 2.8 m deep (Ma et al., 2009). Therefore, the infiltration measured at the base of a conventional  
155 lysimeter may not represent the actual recharge that eventually enters the groundwater system.  
156 Secondly, the measurement accuracy of lysimeter often declines for soils with deep plant roots  
157 because the depth of lysimeter installation is limited and it may be less than the depth of those  
158 roots at site, which by itself can be important pathways for water migration. Consequently, the



159 measured recharge of such disturbed soil by lysimeter may not represent the in-situ recharge of  
160 the native (undisturbed) soil.

161 To resolve the above-mentioned issues faced by the conventional lysimeter, a new type of  
162 lysimeter is designed with specific considerations of the unique precipitation patterns and soil  
163 characteristics in arid and semi-arid regions. This new lysimeter is illustrated schematically in  
164 Figure 1(B).





165

166

167 Figure 1. Schematic diagram of conventional lysimeter (A) and the new lysimeter (B).

## 168 2.2 Design of a new lysimeter for measuring DSR in arid and semi-arid regions

169 This new lysimeter has a few innovations (see Figure 1B) that can be outlined as follows.

170 Instead of setting the upper boundary of the lysimeter at ground surface, the new design has its

171 upper boundary at a designed depth (denoted as depth-A in Figure 1B) where infiltration will be



172 measured. A cylindrical container with a diameter of 20 cm to 40 cm with impermeable walls is  
173 installed from depth-A downward to a deeper depth-B. The length of AB is determined  
174 according to the capillary rise of the in-situ soil, which can be calculated using the average grain  
175 size of soils within AB. More specifically, the length of AB is greater than the capillary rise of  
176 soils within AB and it is usually great than 0.6 m (Liu et al., 2014). At the base of the instrument  
177 (depth B), a water collection device is used to measure the amount of water exit the base.

178 Before the measurement, one necessary preparation is to inject water from the top of the  
179 instrument at depth-A using water pumps, the injection will stop until water starts to drip out  
180 from the base at depth-B. One usually has to wait 10 days to allow the water profile in column  
181 AB to become equilibrium. When water stops flowing out from depth-B, the soil water in the  
182 column is regarded as reaching its equilibrium state, in which the soil moisture at depth-B  
183 reaches the maximum field capacity. Under such an equilibrium status, the amount of infiltration  
184 entering the upper surface of the lysimeter will be discharged (with the same amount) from the  
185 base of the lysimeter after a certain delay time.

186 The proposed new method has a few innovative features that have not been considered in  
187 previous studies. Firstly, it can measure DSR at any given layer of a multi-layer soil system  
188 using a single apparatus installed in the field. Secondly, continuous real-time measurements can  
189 be recorded over any given time period, thus a time-series of DSR can be obtained, which will be  
190 very useful to understand the soil water dynamics at sandy area of arid and semi-arid regions.  
191 Thirdly, the apparatus is portable and easy to install, thus a large amount of data can be collected  
192 in various locations of a study area using multiple lysimeters, and spatial recharge distribution  
193 can also be obtained straightforwardly. This method is field tested in arid and semi-arid sandy  
194 regions of western China. It provides key references for the evaluation of water resources, water

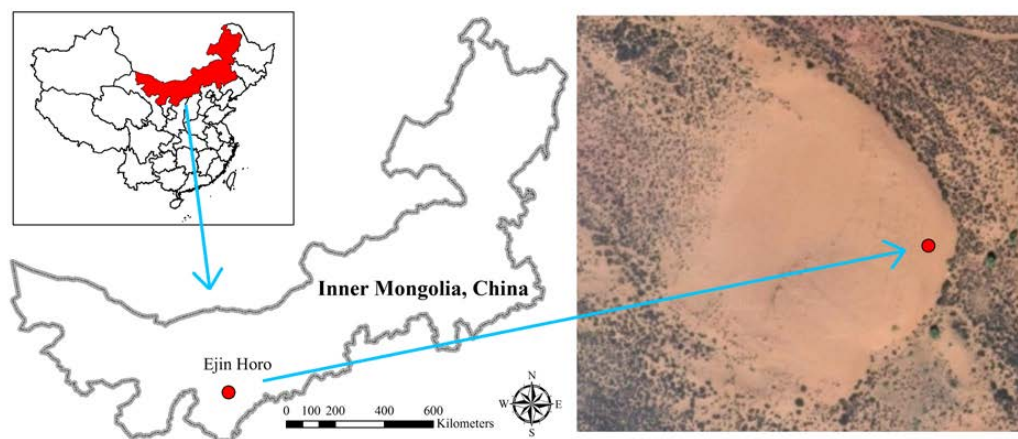


195 balance, and the stability assessment of sand-fixing vegetation in arid and semi-arid areas. It also  
196 provides data that are much needed for evaluating soil water contents and groundwater resources  
197 of those areas. An important feature of this new lysimeter is that it can provide reliable DSR data  
198 to examine the concept of annual recharge coefficient when comparing with the precipitation  
199 data.

### 200 **3. Field testing of the new apparatus**

#### 201 **3.1 Description of the study area**

202 Figure 2 shows the location of the study which is located in Ejin Horo Banner, on the  
203 Eastern margin of Mu Us Sandy Land in the Ordos basin of China (geographic location: 39°05'  
204 N, 109°36' E; altitude: 1070-1556 m above mean sea level). The groundwater table between  
205 dunes are 5.3-6.8 m below ground surface. The climate is semi-arid continental monsoon climate  
206 zone. Precipitation concentrates from July to September, with relatively concentrated rainstorm.  
207 The average annual precipitation from 1960 to 2010 is 296.01 mm. The average annual  
208 temperature of this area is 6.5°C, with about 151 days of frost-free season, 1809 mm total  
209 evaporation, an average 2900 hours of sunshine, and an average wind speed of 3.24 m/s (Wu and  
210 Ci, 2002; Karnieli et al., 2014). The study area is located in relatively gentle mobile dunes, and  
211 the soil type is Aeolian sandy soil.



212



213

214

Figure 2. Geographic location of the experimental area.

215

216

217

218

219

In term of geological structure, Mu Us Sandy Land is in the Ordos basin, a large-scale syncline sedimentary basin with nearly north-south striking axis, and is of Mesozoic and Paleozoic ages. The basin covers an area of 640 km from north to south, and 400 km from east to west. The axis of syncline is off west, and the east and west wings are asymmetric. The east wing is Monoclinic of westward tilt with a width of more than 300 km. The west wing is made of



220 many fault-fold belts striking along the north-south direction and thrusting eastward with a width  
221 of less than 100 km. The southern boundary of the basin is Weibei plateau uplift. The southern  
222 part of this plateau uplift is descending in ladder-shape with blocks to Fenwei rift-subsidence  
223 basin. The northern boundary of this basin is Yimeng plateau uplift, with a lack of Lower  
224 Paleozoic, and its edge-fault is connected to Hetao fault basin. The basement of Ordos basin is of  
225 Precambrian crystalline metamorphic rocks.

226 Deposited in the basin are, in turn, Lower Paleozoic carbonate rocks, Upper Paleozoic-  
227 Mesozoic clastic rocks, and Cenozoic sedimentary rocks with a total depth of more than 6000 m.  
228 The discontinuous Cenozoic sediment is on top of the Mesozoic and Paleozoic layers, mainly of  
229 the Quaternary and partially of the Tertiary sediments. The Quaternary layer is mainly made of  
230 Aeolian sand and loess. Generally divided by a line along the Great Wall, the northwest land  
231 surface is mainly covered by wind-blown sand layers of varying thickness and a 40-120 m thick  
232 layer of alluvial-lacustrine; the southeast land surface is mainly covered by loess with various  
233 thickness from tens of meters to more than 200 m. Below the loess layers, there is Tertiary  
234 Pliocene mud rock with thickness of a few meters to tens of meters.

235 The hydro-stratigraphic units of the Ordos basin is quite complex, consisting of multiple  
236 connected aquifers. Following the order from bottom to top, the multiple aquifers are primarily  
237 made from various rock types of a karst aquifer consisting of Precambrian and Ordovician  
238 limestone, a fractured aquifer consisting of Carboniferous and Jurassic clastic rocks, a porous-  
239 fractured aquifer of Cretaceous clastic rocks, and a porous aquifer consisting of unconsolidated  
240 Cenozoic and Quaternary sediments. Generally speaking, Mu Us Sandy Land has relatively rich  
241 groundwater resources. The shallow groundwater reservoir is estimated to hold about 120.3  
242 billion metric tons of freshwater. Groundwater is mainly recharged by precipitation with an



243 annual average recharge amount of 1.4 billion metric tons. Fine sands are the dominating  
244 sediments observed in the experimental site. In the upper 200 cm soil layer in the experiment  
245 area, the percentage of fine sand (0.5-0.1 mm) are 88.56%, 77.88%, 88.23%, 88.89%, 90.28%,  
246 83.90%, and 84.21% at depths of 0 cm, 10 cm, 30 cm, 60 cm, 90 cm, 150 cm, and 200 cm,  
247 respectively. The rest parts of the soil are primarily coarse sands. It is evident that the soil at the  
248 upper 200 cm is relatively homogeneous.

### 249 **3.2 Statistical analysis of data**

250 Research on the relationship between precipitation and DSR of bare sand land in arid and  
251 semi-arid regions is beneficial to understand the soil-water dynamics of those regions. Because  
252 vegetation is absent, complexity related to transpiration process by plants is not a concern.  
253 Based on two time series of real-time data of precipitation and DSR, one can examine the  
254 relationship between DSR and precipitation. This study can serve as a basis for further study of  
255 DSR in semi-fixed and fixed sand lands with different fractional vegetation covers.

256 The statistics of precipitation and DSR are shown in Table 1, which reveals that there is an  
257 obvious difference of precipitation at the experimental plot from 2013 to 2015. The annual  
258 precipitation is 83 mm in 2013, 205.6 mm in 2014, and 186.4 mm in 2015. This is to say, the  
259 annual precipitations in 2014 and 2015 are 2.48 and 2.25 times of that in 2013, respectively.  
260 Such a dramatic fluctuation and uneven distribution of annual precipitation is typical of arid and  
261 semi-arid regions. The corresponding annual DSR is 20.2 mm in 2013, 20.6 mm in 2014, and 9.2  
262 mm in 2015. This is say that the annual DSR values in 2014 and 2015 are 1.02 and 0.46 of that in  
263 2013. The annual DSR/precipitation ratios (or the so-called annual recharge coefficient) for 2013,  
264 2014, and 2015 are 24.33%, 10%, and 4.94%, respectively.



265 It appears that there is no clear correlation between the annual DSR and the annual  
266 precipitation according to the data of 2013-2015. In another word, use of the annual recharge  
267 coefficient for the study site becomes questionable as such a coefficient implies that there is a  
268 close correlation between the annual DSR and the annual precipitation, which is not supported  
269 by the data of 2013-2015. Therefore, we will scrutinize the precipitation pattern and intensity  
270 more closely to decipher the connection of precipitation and DSR in the following.

271 Table 1: The annual precipitation-DSR relationship from 2013-2015.

Year	Precipitation (mm)	DSR (mm)	DSR/precipitation*100%
2013	83	20.2	24.33%
2014	205.6	20.6	10%
2015	186.4	9.2	4.94%

272

### 273 3.2.1 The relationship between precipitation pattern and DSR

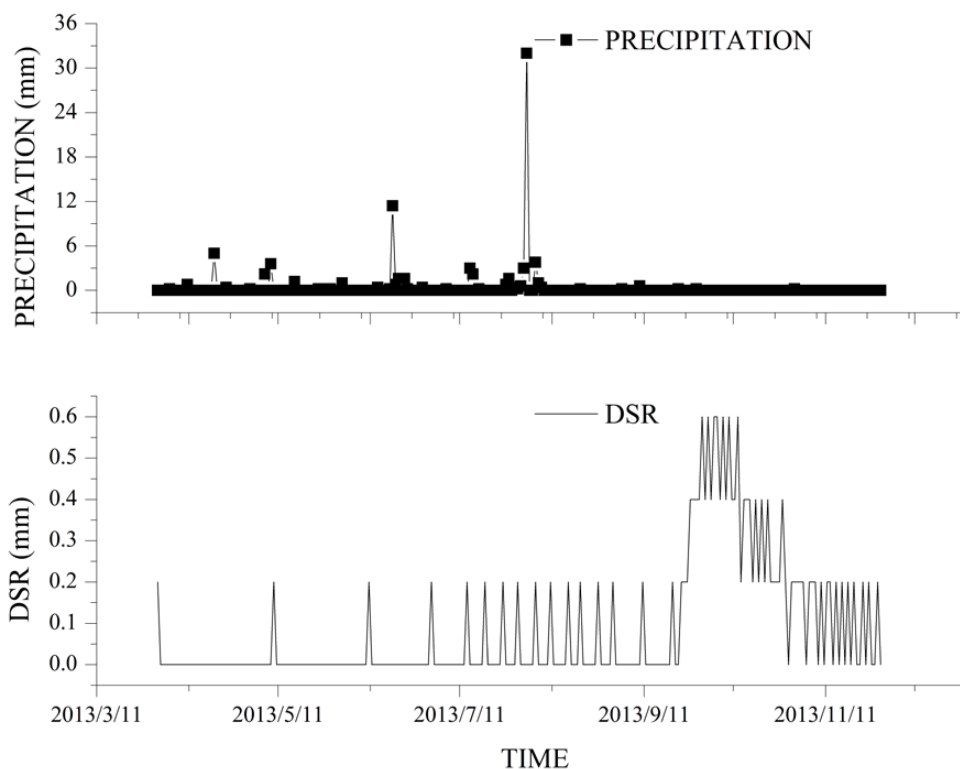
274 Research on bare sandy soil water dynamic process usually focuses on temporal and vertical  
275 differences (Ritsema and Dekker, 1994; Postma et al., 1991). In term of temporal soil moisture  
276 variation over an annual cycle, the process could be divided as soil moisture replenishment,  
277 depletion, and relatively stable periods. In term of vertical soil moisture variation, soil water  
278 content usually first increases with depth and then decreases based on an interplay of mutual  
279 infiltration and evaporation processes. In general, soil could be divided as a surface dry sand  
280 layer, a layer with drastic moisture change, and a layer with relatively stable moisture content.



281 Specifically, the soil deeper than 160 cm in arid and semi-arid regions would have a relatively  
282 stable moisture content. This is because of two reasons. Firstly, soil water will not be up-taken to  
283 the surface by capillary force at such depths; secondly, ground water table in arid and semi-arid  
284 regions is usually much lower than 160 cm.

285 In our study site, 2013 is an especially dry year with only 83 mm precipitation compared to  
286 296.01 mm of average annual rainfall calculated over a period from 1960 to 2010. The  
287 precipitation and DSR patterns of 2013 are shown in Figure 3. The measurement accuracy of the  
288 lysimeter is 0.2 mm. During the observation period from April 1 to November 30, there are  
289 totally 25 recorded precipitation events, mostly concentrated in the period from May to August.  
290 There is a one-time strongest precipitation event with a 24-hour precipitation amount reaching 32  
291 mm in August 3. The DSR correlated to this event can be identified from September 21 to  
292 November 30 and reaches 17.2 mm. The delay time from precipitation event to the start of DSR  
293 is approximately 48 days. The DSR/precipitation ratio for this particular event is as high as  
294 53.75%. Such a DSR/precipitation ratio appears to be the highest in 2013. It is worth to note that  
295 although the strongest precipitation event at August 3 contributes the greatest to DSR observed  
296 from September 21 to November 30, a few precipitation events with amount of 6.6 mm prior to  
297 this strongest precipitation event also contribute a minor part for DSR from July 27 to August 1.  
298 It is also notable that the DSR/precipitation ratio for the strongest precipitation event is  
299 substantially higher than the average annual recharge coefficient of 24.33% in 2013. This leads  
300 to the conclusion that DSR is closely related to the strong precipitation events, rather than to the  
301 average annual precipitation.





302

303

Figure 3: Precipitation and DSR patterns in 2013.

304

305

306

307

308

309

310

311

312

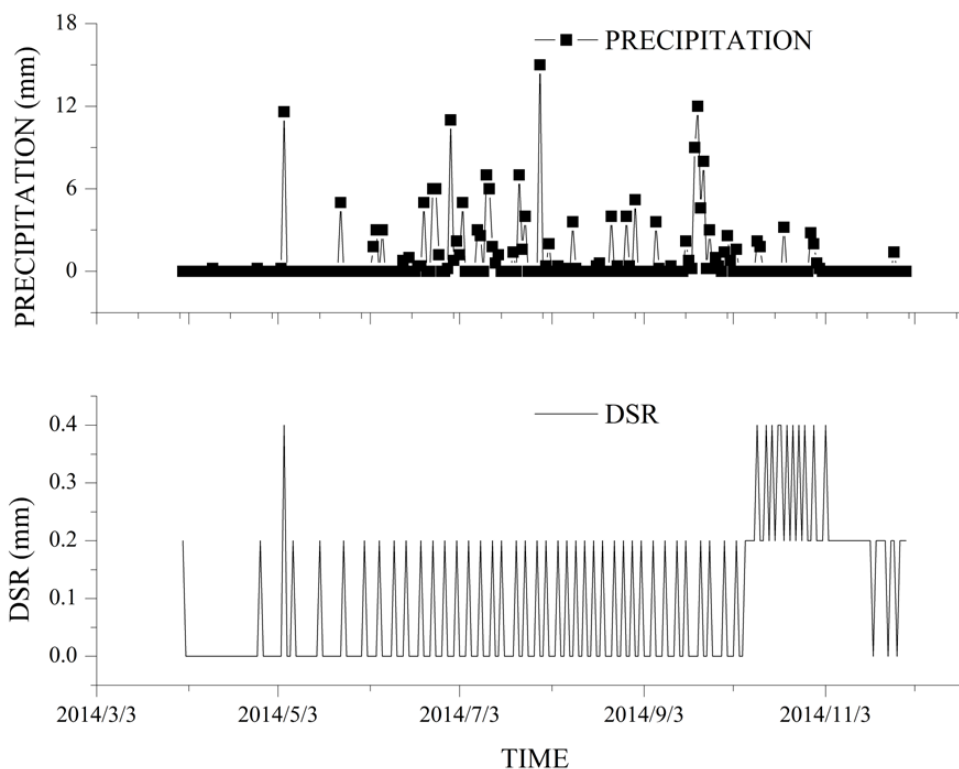
In 2014, the annual precipitation is 205.6 mm, and DSR is 20.6 mm, leading to a 10% annual average recharge coefficient, which is less than half of that in 2013. As shown in Figure 4, the frequency of precipitation events in 2014 is obviously higher than that of 2013. From April 1 to November 30, there are total 68 times of precipitation events, compared to 41 times in 2013. Furthermore, the precipitation distribution in 2014 is more uniform than that in 2013. Specifically, precipitation events are concentrated in the period from June to August, with the highest 24-hour accumulative precipitation of 15 mm on July 30. As shown in Figure 4, recorded DSR data cover a period from April 1 to November 30, and the maximum DSR occurs in October 1. Because the experimental plot is located in a transition zone between arid and semi-



313 arid regions, summer evaporation is strong, leading to relatively less DSR during the summer  
314 season. While during the period from September 1 to November 30, atmospheric temperature  
315 drops and sunshine duration becomes shorter, which results in less surface evaporation and  
316 greater DSR during this period. Compares to 2013, there are more summer precipitation events  
317 in 2014. That is why precipitation in 2014 (205.6 mm) is greater than 2013 (83 mm) but the  
318 overall DSR in 2014 is less than that in 2013.

319 The strongest single-day precipitation in 2014 is 15 mm (occurred in July 30), which is less  
320 than half of the strongest single-day precipitation event of 32 mm occurred in 2013 (August 3),  
321 annual DSR/precipitation ratio of 2013 is 24.33% but in 2014 is 10%. This once again supports  
322 the conclusion that the strong precipitation events rather than the average annual precipitation are  
323 mostly responsible for the average annual DSR.

324



325

326

Figure 4: Precipitation and DSR patterns in 2014.

327

328

329

330

331

332

333

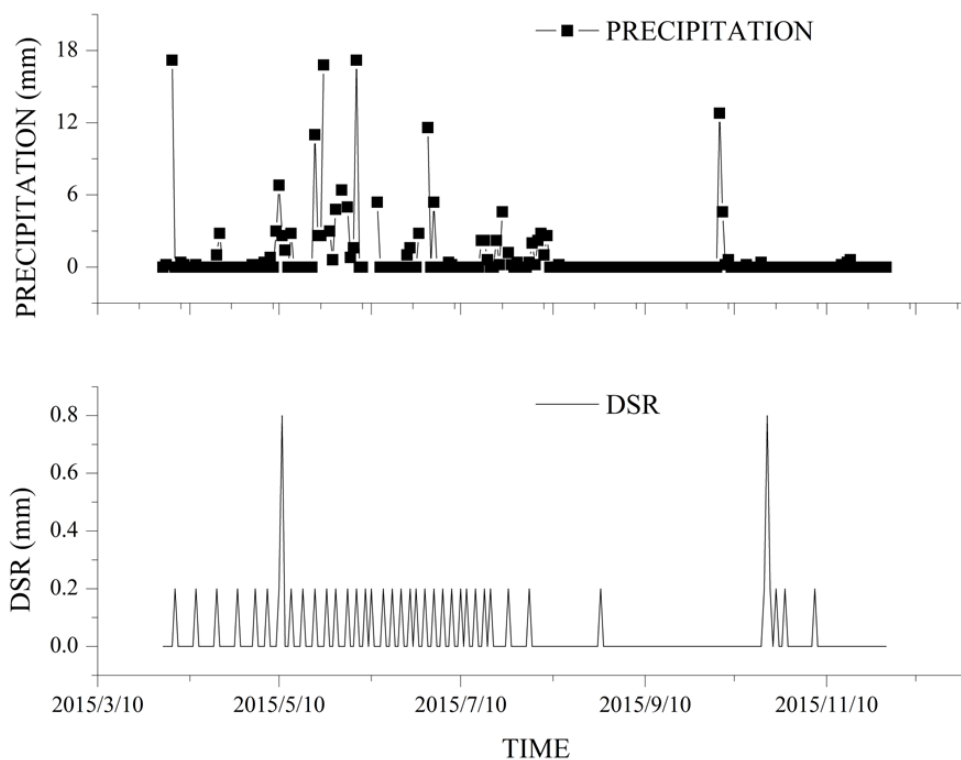
334

335

As shown in Figure 5, the total annual precipitation of 2015 is 186.4 mm, and DSR is 9.2 mm, leading to a 4.94% annual average recharge coefficient, which is significantly smaller than of 2013 (24.33%) and 2014 (10%). There are total 66 observable precipitation events in 2015. Such precipitation events are mostly concentrated from April 4 to July 6, with a total precipitation of 155 mm during this period, which represents 83.15% of the total precipitation in 2015. The measured DSR from April 4 to July 6 is only 7 mm, representing 77.78% of the total DSR in 2015. Throughout 2015, two strongest precipitation events happens on April 4 and June 5, both 24-hour precipitation events reach 17.2 mm. We observe a single-day DSR peak of 0.8 mm 36 days after April 4, one of the two greatest single-day DSR values observed in 2015, but



336 no peak value of DSR response to the strong precipitation in June 5. As explained before,  
337 summer stronger evaporation leads to relatively less DSR during the summer season compared  
338 with other seasons. The third greatest precipitation is 16.8 mm in October 5, which leads to a  
339 peak value of 0.8 mm of DSR in October 21, with a 16-day delay time. If comparing the  
340 precipitation events occurred in April 4 (17.2 mm) and October 5 (16.8 mm), one can see that  
341 these two precipitation events are similar in strength (17.2 mm for April 4 and 16.8 mm for  
342 October 5) but different in the DSR delay time (36 days for April 4 and 16 days for October 5).  
343 This lead to a conclusion that temperature influences the DSR rate. To investigate how the soil  
344 temperature affects the DSR rate, further field experiments are needed in the future study.



345

346

Figure 5: Precipitation and DSR patterns in 2015.



### 347 **3.2.2 Relationship between precipitation intensity and DSR**

348 Based on observational data and analysis in 3.2.1, one can see that precipitation intensity, to  
349 some extent, influences DSR. For the sake of illustration, the precipitation intensity for bare sand  
350 land is roughly classified into light, moderate, and strong events with precipitation amount less  
351 than 6 mm, between 6 mm to 10 mm, and greater than 10 mm, respectively. In general, light  
352 precipitation rarely can reach the soil zone deeper than 40 cm because of evaporation, thus it  
353 makes almost no contribution to DSR (Zhang et al., 2016). Such a classification may be revised  
354 under different vegetation covering conditions in different regions (Kosmas et al., 2000).

355 According to this classification, statistics of moderate to strong precipitation events and  
356 their percentage shares in the annual precipitation from 2013 to 2015 are shown in Table 2. In  
357 2013, there are only two precipitation events with intensity greater than 6 mm. The total amount  
358 of these two precipitation events is 43.4 mm, which represents 52.29% of the annual  
359 precipitation in 2013. In 2014, there are 11 precipitation events with intensity greater than 6 mm,  
360 much more frequent than that of 2013 (2 times) and moderately more frequent than that of 2015  
361 (8 times). The total moderate to strong precipitation in 2014 is 98.6 mm, representing 47.96% of  
362 the annual precipitation in 2014. In 2015, there are 8 precipitation events with intensity greater  
363 than 6 mm, accounting for 53.54% of the annual precipitation in 2015.

364 Among these three years, 2015 has the largest percentage of moderate to strong  
365 precipitation over the annual precipitation. However, at this same year, one has seen the smallest  
366 ratio of annual DSR/precipitation ratio or annual recharge coefficient (see Table 1). This implies  
367 that the annual DSR does not seem to be positively correlated to the annual total precipitation.  
368 This finding has a few profound consequences. It basically states that assigning a constant annual  
369 recharge coefficient for a particular soil regardless of precipitation patterns is not a good practice,



370 because annual DSR is not always proportional to the total annual precipitation. Instead, it  
 371 appears to be more closely related to individual precipitation events stronger than 10 mm.

372 Table 2: Percentage of valid precipitation in total precipitation amount.

Year	Number of precipitation >6mm (24 hr cumulative)	Amount of precipitation >6mm (mm)	Valid precipitation /annual precipitation (%)
2013	2	43.4	52.29
2014	11	98.6	47.96
2015	8	99.8	53.54

373

374 Table 3 lists the number of strong precipitation (with amount greater than 10 mm) and also  
 375 the strongest precipitation amount for each of 2013, 2014 and 2015. In 2013, there are only 2  
 376 strong precipitation events, but the maximum single-day precipitation amount reaches 32 mm  
 377 (August 3). The accumulative strong precipitation of 2013 is 43.4 mm, which is 52.28% of the  
 378 annual precipitation in 2013. In 2014, there are 4 strong precipitation events and the maximum  
 379 single-day precipitation amount is 15 mm. The accumulative strong precipitation of 2014 is 49.6  
 380 mm, which is 24.12% of the annual precipitation in 2014. In 2015, there are 6 strong  
 381 precipitation events, and the maximum single-day precipitation amount is 17.2 mm. The  
 382 accumulative strong precipitation of 2015 is 86.6 mm, which represents 46.46% of the annual  
 383 precipitation in 2015. The annual DSR versus annual precipitation ratios are 24.33%, 10%, and  
 384 4.94% for 2013, 2014, and 2015, respectively.



385 As shown in Table 3, the strongest single-day precipitation (32 mm in 2013) appears to  
 386 affect DSR the most in 2013. For 2014 and 2015, as the strongest precipitation events in these  
 387 two years (15 mm and 17.2 mm, respectively) are significantly smaller than that in 2013, the  
 388 correlation between annual DSR and the strongest precipitation events for these two years  
 389 becomes less significant. In summary, one may conclude that annual DSR in arid and semi-arid  
 390 regions mainly rely on strong precipitation events, but the determination of the threshold for  
 391 strong precipitation events that directly contribute to DSR is still unclear and requires further  
 392 investigation.

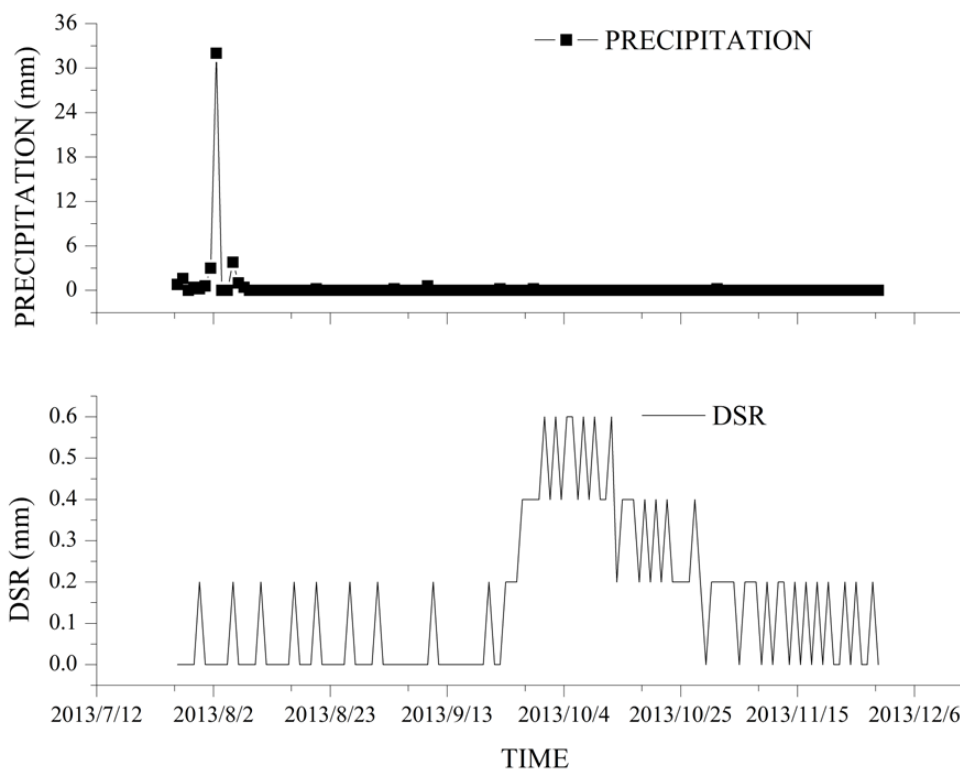
393 Table 3: Inter-annual statistics of strong precipitation and its percentage in total annual  
 394 precipitation amount.

Year	Number of strong precipitation event	Maximum precipitation event (mm)	Cumulative strong precipitation amount (mm)	Percentage in total annual precipitation amount (%)	Annual DSR (mm)	Annual DSR /annual precipitation (%)
2013	2	32	43.4	52.28	20.2	24.33
2014	4	15	49.6	24.12	20.6	10
2015	6	17.2	86.6	46.46	9.2	4.94

395



396 Under the condition of continuous precipitation, it may be difficult to discretize  
397 precipitation into individual events. The following example illustrates a procedure to deal with  
398 this situation. As shown in Figure 6, there is a 13-days continuous precipitation process in 2013  
399 from July 27 to August 8, and the accumulative precipitation is 43.8 mm. The start of a  
400 continuous DSR distribution corresponding to this 13-day continuous precipitation event is  
401 observed 3 days after the end of this precipitation process, and the peak value of DSR occurs 46  
402 days after the end of this precipitation process. The DSR distribution gradually recedes to zero  
403 around 78 days after the end of the precipitation process. The accumulative DSR amount over a  
404 75-day period is 18.4 mm. The ratio of the 75-day cumulative DSR over the 13-day precipitation  
405 event is 42%.



406  
407

Figure 6: One-day intensive precipitation's contribution to DSR in 2013.





408 **4. Discussion**

409 This improved lysimeter is on the real-time dynamic monitoring of DSR, and it provides  
410 reliable evidence for an accurate evaluation of precipitation-related recharging capability of bare  
411 sand lands in arid and semi-arid regions. However, there are a number of issues that deserves  
412 further attention and requires additional investigations in the future. The moisture evaporation,  
413 the soil absorption of moisture, and the water infiltration of post-evaporative redistribution, are  
414 all very complex processes, especially in arid and semi-arid regions. It is sometimes difficult to  
415 clearly distinguish the amount of evaporation and DSR with conventional methods as outlined in  
416 the introduction. This study selects precipitation and infiltration data during the period from  
417 April 1 to November 30, so the influence of freeze-thaw process during winter is avoided, and  
418 the experimental design and data analysis is simplified. For this reasons, the next steps should be  
419 a full-term monitoring, a systematic study on DSR, as well as a study on the soil temperature and  
420 daily temperature influences on DSR.

421 Although this experiment does not address the issue of soil temperature effect on DSR in  
422 great details, the relationship between DSR and soil temperature is evident. In general, a higher  
423 temperature means a stronger evaporation demand, thus an often smaller DSR.

424 Through the analysis of this study, one can see that the use of an annual recharge coefficient  
425 for the study area is not supported by the data collected from the new lysimeter, as the annual  
426 recharge is not positively correlated with the annual total precipitation. Instead, we find that the  
427 recharge is somewhat positively correlated with a few strong precipitation events (greater than  
428 10 mm), and very closely correlated with the strongest precipitation event (considerably greater  
429 than 10 mm). It is probably reasonable to assign different weighting factors for different  
430 precipitation strengths to calculate DSR. However, the threshold to define a strong precipitation



431 event that makes direct contribution to DSR is not precisely quantified, and this is a subject that  
432 should be investigated in more details in the future. The determination of weighting factors for  
433 different precipitation strengths is also a subject requires further investigation.

434

## 435 **5. Conclusions**

436 This study uses a newly designed lysimeter to study three consecutive years (2013-2015) of DSR  
437 underneath bare sand land on the Eastern margin of Mu Us Sandy Land in the Ordos basin of  
438 China. The objective is to identify the characteristics of the DSR distribution and the factors  
439 affecting the DSR distribution. Specifically, we like to examine if the commonly used recharge  
440 coefficient concept can be applied for arid and semi-arid regions such as the Eastern margin of  
441 Mu Us Sandy Land of China.

442 The following conclusions can be drawn from this study:

443 (1) The annual recharge coefficient concept is generally inapplicable for estimating DSR in the  
444 study site.

445 (2) Precipitation pattern including precipitation intensity and precipitation season significantly  
446 influences DSR.

447 (3) The temperature influences the DSR/precipitation ratio, which is less in summer as in other  
448 seasons, given the similar precipitation intensity.

449 (4) DSR is not correlated with the annual precipitation. Instead, it is correlated with the strong  
450 precipitation (greater than 10 mm) events at the site. However, quantitative determination of  
451 the thresholds for such strong precipitation events that makes direct contribution to DSR is  
452 not entirely understood. Further investigation is needed on this subject.

453



454 **Acknowledgements.** This study was supported with research grants from the Ministry of  
455 Science and Technology of the People's Republic of China (2013CB429901).

456

457 **References**

458

459 Acworth, R. I., Rau, G. C., Cuthbert, M. O., Jensen, E., and Leggett, K.: Long-term spatio-temporal  
460 precipitation variability in arid-zone Australia and implications for groundwater recharge, *Hydrogeology*  
461 *Journal*, 24, 905-921, 2016.

462 Adolph, E. F.: *Physiology of Man in the Desert*, Physiology of Man in the Desert., 1947.

463 Allison, G., Gee, G., and Tyler, S.: Vadose-zone techniques for estimating groundwater recharge in arid  
464 and semiarid regions, *Soil Science Society of America Journal*, 58, 6-14, 1994.

465 Allocca, V., Manna, F., and De Vita, P.: Estimating annual groundwater recharge coefficient for karst  
466 aquifers of the southern Apennines (Italy), *Hydrology and Earth System Sciences*, 18, 803, 2014.

467 Arnold, J. G., Moriasi, D. N., Gassman, P. W., Abbaspour, K. C., White, M. J., Srinivasan, R., Santhi, C.,  
468 Harmel, R., Van Griensven, A., and Van Liew, M. W.: SWAT: Model use, calibration, and validation,  
469 *Transactions of the ASABE*, 55, 1491-1508, 2012.

470 Beatley, J. C.: Phenological events and their environmental triggers in Mojave Desert ecosystems,  
471 *Ecology*, 55, 856-863, 1974.

472 Collins, S. L., Belnap, J., Grimm, N., Rudgers, J., Dahm, C. N., D'odorico, P., Litvak, M., Natvig, D., Peters, D.  
473 C., and Pockman, W.: A multiscale, hierarchical model of pulse dynamics in arid-land ecosystems, *Annual*  
474 *Review of Ecology, Evolution, and Systematics*, 45, 397-419, 2014.

475 Duncan, M., Srinivasan, M., and McMillan, H.: Field measurement of groundwater recharge under  
476 irrigation in Canterbury, New Zealand, using drainage lysimeters, *Agricultural Water Management*, 166,  
477 17-32, 2016.

478 Farahani, H., Howell, T., Shuttleworth, W., and Bausch, W.: Evapotranspiration: progress in  
479 measurement and modeling in agriculture, *Trans. Asabe*, 50, 1627-1638, 2007.

480 Fayer, M. J.: UNSAT-H version 3.0: Unsaturated soil water and heat flow model. Theory, user manual,  
481 and examples, Pacific Northwest National Laboratory, 13249, 2000.

482 Fiorillo, F., Pagnozzi, M., and Ventafridda, G.: A model to simulate recharge processes of karst massifs,  
483 *Hydrological Processes*, 29, 2301-2314, 2015.

484 Fritzsche, A., Pagels, B., and Totsche, K. U.: The composition of mobile matter in a floodplain topsoil: A  
485 comparative study with soil columns and field lysimeters, *Journal of Plant Nutrition and Soil Science*, 179,  
486 18-28, 2016.

487 Gee, G. W., and Hillel, D.: Groundwater recharge in arid regions: review and critique of estimation  
488 methods, *Hydrological Processes*, 2, 255-266, 1988.

489 Glenn, E. P., Anday, T., Chaturvedi, R., Martinez-Garcia, R., Pearlstein, S., Soliz, D., Nelson, S. G., and  
490 Felger, R. S.: Three halophytes for saline-water agriculture: An oilseed, a forage and a grain crop,  
491 *Environmental and Experimental Botany*, 92, 110-121, 2013.

492 Goldhamer, D. A., Fereres, E., Mata, M., Girona, J., and Cohen, M.: Sensitivity of continuous and discrete  
493 plant and soil water status monitoring in peach trees subjected to deficit irrigation, *Journal of the*  
494 *American Society for Horticultural Science*, 124, 437-444, 1999.

495 Good, S. P., Noone, D., and Bowen, G.: Hydrologic connectivity constrains partitioning of global  
496 terrestrial water fluxes, *Science*, 349, 175-177, 2015.

497 Hickel, K., and Zhang, L.: Estimating the impact of rainfall seasonality on mean annual water balance  
498 using a top-down approach, *Journal of Hydrology*, 331, 409-424, 2006.



- 499 Howell, T. A., Schneider, A. D., and Jensen, M. E.: History of lysimeter design and use for  
500 evapotranspiration measurements, *Lysimeters for Evapotranspiration and Environmental*  
501 *Measurements*, 1991, 1-9,
- 502 Huxman, T. E., Snyder, K. A., Tissue, D., Leffler, A. J., Ogle, K., Pockman, W. T., Sandquist, D. R., Potts, D.  
503 L., and Schwinning, S.: Precipitation pulses and carbon fluxes in semiarid and arid ecosystems, *Oecologia*,  
504 141, 254-268, 2004.
- 505 Jiménez-Martínez, J., Candela, L., Molinero, J., and Tamoh, K.: Groundwater recharge in irrigated semi-  
506 arid areas: quantitative hydrological modelling and sensitivity analysis, *Hydrogeology Journal*, 18, 1811-  
507 1824, 2010.
- 508 Kalbus, E., Reinstorf, F., and Schirmer, M.: Measuring methods for groundwater? surface water  
509 interactions: a review, *Hydrology and Earth System Sciences Discussions*, 10, 873-887, 2006.
- 510 Karnieli, A., Qin, Z., Wu, B., Panov, N., and Yan, F.: Spatio-temporal dynamics of land-use and land-cover  
511 in the Mu Us sandy land, China, using the change vector analysis technique, *Remote Sensing*, 6, 9316-  
512 9339, 2014.
- 513 Katz, B. S., Stotler, R. L., Hirmas, D., Ludvigson, G., Smith, J. J., and Whittemore, D. O.: Geochemical  
514 Recharge Estimation and the Effects of a Declining Water Table, *Vadose Zone Journal*, 15, 2016.
- 515 Klaus, J., and McDonnell, J.: Hydrograph separation using stable isotopes: review and evaluation, *Journal*  
516 *of Hydrology*, 505, 47-64, 2013.
- 517 Kosmas, C., Danalatos, N., and Gerontidis, S.: The effect of land parameters on vegetation performance  
518 and degree of erosion under Mediterranean conditions, *Catena*, 40, 3-17, 2000.
- 519 Krysanova, V., Hattermann, F., and Wechsung, F.: Development of the ecohydrological model SWIM for  
520 regional impact studies and vulnerability assessment, *Hydrological Processes*, 19, 763-783, 2005.
- 521 Li, X., Zhang, Z., Tan, H., Gao, Y., Liu, L., and Wang, X.: Ecological restoration and recovery in the wind-  
522 blown sand hazard areas of northern China: relationship between soil water and carrying capacity for  
523 vegetation in the Tengger Desert, *Science China. Life Sciences*, 57, 539, 2014.
- 524 Li, X. R., Ma, F. Y., Xiao, H. L., Wang, X. P., and Kim, K. C.: Long-term effects of revegetation on soil water  
525 content of sand dunes in arid region of Northern China, *Journal of Arid Environments*, 57, 1-16, 2004.
- 526 Liu, Q., Yasufuku, N., Miao, J., and Ren, J.: An approach for quick estimation of maximum height of  
527 capillary rise, *Soils and Foundations*, 54, 1241-1245, 2014.
- 528 Ma, J., Ding, Z., Edmunds, W. M., Gates, J. B., and Huang, T.: Limits to recharge of groundwater from  
529 Tibetan plateau to the Gobi desert, implications for water management in the mountain front, *Journal of*  
530 *Hydrology*, 364, 128-141, 2009.
- 531 McWhorter, D. B., and Sunada, D. K.: Ground-water hydrology and hydraulics, *Water Resources*  
532 *Publication*, 1977.
- 533 Min, L., Shen, Y., Pei, H., and Jing, B.: Characterizing deep vadose zone water movement and solute  
534 transport under typical irrigated cropland in the North China Plain, *Hydrological Processes*, 2017.
- 535 Modarres, R., and da Silva, V. d. P. R.: Rainfall trends in arid and semi-arid regions of Iran, *Journal of Arid*  
536 *Environments*, 70, 344-355, 2007.
- 537 Nyman, P., Sheridan, G. J., Smith, H. G., and Lane, P. N.: Modeling the effects of surface storage,  
538 macropore flow and water repellency on infiltration after wildfire, *Journal of Hydrology*, 513, 301-313,  
539 2014.
- 540 Ogle, K., and Reynolds, J. F.: Plant responses to precipitation in desert ecosystems: integrating functional  
541 types, pulses, thresholds, and delays, *Oecologia*, 141, 282-294, 2004.
- 542 Postma, D., Boesen, C., Kristiansen, H., and Larsen, F.: Nitrate reduction in an unconfined sandy aquifer:  
543 water chemistry, reduction processes, and geochemical modeling, *Water Resources Research*, 27, 2027-  
544 2045, 1991.
- 545 Ritsema, C. J., and Dekker, L. W.: How water moves in a water repellent sandy soil: 2. Dynamics of  
546 fingered flow, *Water Resources Research*, 30, 2519-2531, 1994.



- 547 Sanford, W.: Recharge and groundwater models: an overview, *Hydrogeology Journal*, 10, 110-120, 2002.
- 548 Scanlon, B. R.: Evaluation of methods of estimating recharge in semiarid and arid regions in the  
549 southwestern US, *Groundwater recharge in a desert environment: The southwestern United States*, 235-  
550 254, 2013.
- 551 Schymanski, S. J., Sivapalan, M., Roderick, M., Beringer, J., and Hutley, L.: An optimality-based model of  
552 the coupled soil moisture and root dynamics, *Hydrology and Earth System Sciences Discussions*, 12, 913-  
553 932, 2008.
- 554 Shou, W., Musa, A., Liu, Z., Qian, J., Niu, C., and Guo, Y.: Rainfall partitioning characteristics of three  
555 typical sand-fixing shrubs in Horqin Sand Land, north-eastern China, *Hydrology Research*, nh2016177,  
556 2016.
- 557 Šimůnek, J., Van Genuchten, M. T., and Šejna, M.: HYDRUS: Model use, calibration, and validation, *Trans.*  
558 *Asabe*, 55, 1261-1274, 2012.
- 559 Soyly, M., Istanbuloglu, E., Lenters, J., and Wang, T.: Quantifying the impact of groundwater depth on  
560 evapotranspiration in a semi-arid grassland region, *Hydrology and Earth System Sciences*, 15, 787-806,  
561 2011.
- 562 Stessel, R., and Murphy, R.: A lysimeter study of the aerobic landfill concept, *Waste Management &*  
563 *Research*, 10, 485-503, 1992.
- 564 Turkeltaub, T., Kurtzman, D., Bel, G., and Dahan, O.: Examination of groundwater recharge with a  
565 calibrated/validated flow model of the deep vadose zone, *Journal of Hydrology*, 522, 618-627, 2015.
- 566 van Dam, J. C.: Field-scale water flow and solute transport: SWAP model concepts, parameter estimation  
567 and case studies, [sn], 2000.
- 568 Vauclin, M., Khanji, D., and Vachaud, G.: Experimental and numerical study of a transient,  
569 two-dimensional unsaturated-saturated water table recharge problem, *Water Resources Research*, 15,  
570 1089-1101, 1979.
- 571 Voeckler, H. M., Allen, D. M., and Alila, Y.: Modeling coupled surface water–Groundwater processes in a  
572 small mountainous headwater catchment, *Journal of Hydrology*, 517, 1089-1106, 2014.
- 573 Weihermüller, L., Siemens, J., Deurer, M., Knoblauch, S., Rupp, H., Göttlein, A., and Pütz, T.: In situ soil  
574 water extraction: a review, *Journal of environmental quality*, 36, 1735-1748, 2007.
- 575 Williams, W. D.: Salinisation: A major threat to water resources in the arid and semi-arid regions of the  
576 world, *Lakes & Reservoirs: Research & Management*, 4, 85-91, 1999.
- 577 Wu, B., and Ci, L. J.: Landscape change and desertification development in the Mu Us Sandland,  
578 Northern China, *Journal of Arid Environments*, 50, 429-444, 2002.
- 579 Zhang, J., Felzer, B. S., and Troy, T. J.: Extreme precipitation drives groundwater recharge: the Northern  
580 High Plains Aquifer, central United States, 2016.
- 581 Zhang, L., Dawes, W., and Walker, G.: Response of mean annual evapotranspiration to vegetation  
582 changes at catchment scale, *Water resources research*, 37, 701-708, 2001.
- 583 Zhang, Y., Kendy, E., Qiang, Y., Changming, L., Yanjun, S., and Hongyong, S.: Effect of soil water deficit on  
584 evapotranspiration, crop yield, and water use efficiency in the North China Plain, *Agricultural Water*  
585 *Management*, 64, 107-122, 2004.
- 586 Zhou, J., Fu, B., Gao, G., Lü, Y., Liu, Y., Lü, N., and Wang, S.: Effects of precipitation and restoration  
587 vegetation on soil erosion in a semi-arid environment in the Loess Plateau, China, *Catena*, 137, 1-11,  
588 2016.
- 589